JOURNAL OF PROPULSION AND POWER
Vol. 27, No. 2, March–April 2011

Robust Design Optimization of Gas Turbine Compression Systems

Tiziano Ghisu,* Geoffrey T. Parks,† Jerome P. Jarrett,‡ and P. John Clarkson§
Cambridge University, Cambridge, England CB2 1PZ, United Kingdom

DOI: 10.2514/1.48965

Gas turbine compression systems are required to perform adequately over a range of operating conditions. Complexity has encouraged the conventional design process for compressors to focus initially on one operating point, usually the most common or arduous, to draw up an outline design. Generally, only as this initial design is refined is its offdesign performance assessed in detail. Not only does this necessarily introduce a potentially costly and time-consuming extra loop in the design process, but it also may result in a design whose offdesign behavior is suboptimal. A version of nonintrusive polynomial chaos was previously developed in which a set of orthonormal polynomials was generated to facilitate a rapid analysis of robustness in the presence of generic uncertainties with good accuracy. In this paper, this analysis method is incorporated in real time into the design process for the compression system of a three-shaft gas turbine aeroengine. This approach to robust optimization is shown to lead to designs that exhibit consistently improved system performance with reduced sensitivity to offdesign operation.

Nomenclature

DF	=	diffusion factor
DH	=	de Haller number
H	=	boundary-layer shape factor
I_i	=	generic Wiener–Askey polynomial
L	=	length
$\bar{m}$	=	(pseudo) nondimensional mass-flow rate
$\dot{m}$	=	mass-flow rate
N	=	number of random dimensions
N_t	=	number of collocation points
N_0	=	quadrature order
P	=	pressure
PR	=	pressure ratio
p	=	polynomial chaos order
R	=	radius
SM	=	surge margin
SPR	=	static-pressure-rise coefficient
T	=	temperature
W	=	weighting function
$\dot{W}$	=	power
w	=	weight factor
Y	=	random process
y_i	=	random process' expansion coefficient
γ	=	ratio of specific heats
δ_{ij}	=	Kronecker delta
η	=	isentropic efficiency
Θ_i	=	multivariate polynomial, a product of one-dimensional orthonormal polynomials
μ	=	mean value
$\boldsymbol{\xi}$	=	vector of support random variables
ξ_i	=	support random variable
Π_i	=	multidimensional adaptive orthonormal polynomial
σ^2	=	variance
τ_i	=	input uncertainty
Υ	=	random variables' space
Φ_i	=	Wiener–Askey chaos
ω	=	duct total pressure loss (fraction of inlet)

Subscript

0	=	total (stagnation) conditions

Received 20 January 2010; revision received 23 August 2010; accepted for publication 23 November 2010.

*Research Associate, Engineering Design Centre, Engineering Department, Trumpington Street.

†Senior Lecturer, Engineering Design Centre, Engineering Department, Trumpington Street.

‡University Lecturer, Engineering Design Centre, Engineering Department, Trumpington Street. Member AIAA.

§Professor, Engineering Design Centre, Engineering Department, Trumpington Street.

I. Introduction

A COMMON simplification in the design process for any engineering system is to assume nominal values for a number of design parameters (ranging from operating conditions to manufacturing tolerances, damage processes, and so on). Although these assumptions are often essential to make the design process tractable, they may lead to products that in real-world environments exhibit significant deviations from their nominal performance. This problem is often exacerbated in heavily optimized products, which tend to lie in extreme regions of the design space [1].

For gas turbine engines (and compression systems more specifically) the nominal design point is usually chosen to be the point with the severest conditions or the strongest influence on the figures of merit: this is generally a high-speed condition with high nondimensional mass flow and rotational speed (often top of climb) [2]. However, as the engine, during its normal operation, is expected to work over a significant range of throttle settings (such as engine starting, idling, reduced power, and maximum thrust), satisfactory performance and safe operation must be guaranteed for all the possible working conditions [3]. Offdesign performance is usually assessed after the preliminary design phase (the more advanced the project is, the more complex it becomes to modify any fundamental design choices).

This approach, although guaranteeing that some minimum offdesign performance requirements are met, introduces a further loop in the design process, thus adding a further level of hierarchicality and fragmentation. Moreover, there might be a substantial difference between satisfactory and optimal performance, and heavy optimization of some design-point figures of merit might actually be detrimental to the overall performance. A tighter integration of robustness considerations into the design process can reduce the degree of decomposition that is typical of gas turbine design and, potentially, produce a design solution with improved performance over a range of operating conditions rather than just at a particular operating point, albeit the most important one.

In previous work [4], the authors proposed a method for propagating generic uncertainties through a system and demonstrated its applicability and reliability in the analysis of the variability

in performance of a core compression system from a three-spool gas turbine engine. The reasonable computational cost of the method, based on a nonintrusive polynomial chaos formulation, suggests it would be practical to integrate it within the design process, with the dual aims of reducing the fragmentation of the process and of facilitating the identification of design solutions less sensitive to the presence of design or operational uncertainties.

In this work, the proposed uncertainty analysis method is used first to analyze the sensitivity in the presence of three uncertain parameters (representing engine throttle, air bleed and power offtake) of designs obtained from a traditional design-point optimization (previously presented by the authors [5,6]). This analysis allows configurations with satisfactory offdesign performance to be isolated. The uncertainty analysis method is then directly integrated within the design optimization loop itself; this results in the identification of solutions that further improve the overall performance of the system and are also intrinsically less sensitive to the presence of the given uncertain parameters.

II. Background

A. Robust Aerodynamic Optimization

Despite the extensive application of optimization techniques in aerodynamic design [1], few studies approach this problem from a statistical point of view; the high cost of aerodynamic simulations undoubtedly complicates the application of robust design methodologies. Only in recent years has the availability of ever more powerful computers (and more efficient evaluation tools) made exploration of this approach possible.

Huyse et al. [7] use a statistical approach in the design of 2-D airfoils. They use a deterministic optimizer to improve the performance of an airfoil with 21 degrees of freedom, attempting to minimize the drag coefficient for a given distribution of the flight Mach number. They recognize the high cost of running several computations under different operating conditions and the need for a computational scheme that minimizes the number of evaluation calls. The mean value of the drag coefficient is automatically calculated for the specific Mach number distribution using a four-point quadrature formula, obtained by random selection of the integration points to make the solution independent of the particular integration points.

Putko et al. [8] apply a moment method to the propagation of input uncertainties through a 1-D Euler computational fluid dynamics (CFD) code. Mean and variance of the objective function are calculated based on the input noise factors' statistics and on the first- and second-order derivatives of the objective function with respect to the noise factors themselves. The derivatives are calculated efficiently with ADIFOR 3.0, a tool for automatic differentiation based on the adjoint formulation of the governing equations [9]. A gradient-based optimizer is then used to locate the optimal design of a nozzle, for uncertainties in either the geometrical characteristics or the flow properties. The same authors [10] use a first-order moment method in the optimization of the lift of a 2-D airfoil for uncertain input CFD parameters.

Gumbert et al. [11] use the same approach for the multidisciplinary (aerodynamic and structural) optimization of a 3-D wing. They use a gradient-based optimizer in the robust optimization of the wing with noisy geometric parameters, treating a weighted sum of mean lift-to-drag ratio and mass as the objective and its variance as a constraint.

Poloni et al. [12] use game theory in the multiobjective optimization of a transonic airfoil under uncertain Mach number and angle of attack. Mean and variance of the drag coefficient are optimized simultaneously. A kriging response surface is built based on the results of a viscous CFD solver to minimize computational times.

The authors are aware of three works that consider the effect of uncertainties on compressor performance. The first, by Garzon and Darmofal [13], analyzes the effect of variability in the geometry of a rotor blade (measured from 200 actual blades) on flow turning and loss coefficient by means of Monte Carlo simulation (MCS), using a throughflow solver. Garzon and Darmofal include the model in the analysis of a six-stage compressor, computing a 1.2% variability in efficiency, but do not perform an optimization.

Lian and Kim [14] analyze the effect of uncertainties in material properties in the optimization of a transonic rotor blade to minimize weight and maximize stage pressure ratio, satisfying aerodynamic and structural constraints. They use a genetic algorithm to drive the optimization and a second-order response surface coupled with MCS to propagate the input uncertainties through the system, obtaining improved performance, reduced weight and a more reliable design.

Another interesting study of robust design is by Kumar et al. [15], who optimize the 2-D design of a blade against erosion. They use 10 Hicks and Henne functions [16] to parameterize the design space and a further one to describe the erosion pattern. Three probabilistic parameters influence the location, depth and width of the eroded section. A multiobjective genetic algorithm drives the design process, aiming simultaneously at maximizing the mean blade pressure loss and at minimizing its standard deviation. A kriging surrogate model is used both to accelerate the search and to reduce the number of function evaluations necessary for the uncertainty estimation, which is based on MCS performed on the kriging model produced after a 50-point LP-τ survey [17]. Keane [18] expands on this work, dealing with geometrical variations due to manufacturing errors and foreign object damage. He uses a 15-point LP-τ survey to estimate the variability in performance caused by the given uncertainties, using both a worst-case method and an expected improvement approach to drive the robust optimization process.

B. Polynomial Chaos

The roots of polynomial chaos (PC) are to be found in the homogeneous chaos expansion first proposed by Wiener [19], who employed Hermite polynomials in terms of Gaussian random variables to express stochastic processes with finite variance. Cameron and Martin [20] demonstrated that "any Fourier-Hermite series of any functional $F(x)$ of $L_2(C)$ converges in the $L_2(C)$ sense to $F(x)$" (i.e., any variable with finite variance, or second-order, can be represented exactly through the above-mentioned homogeneous chaos expansion). The natural application is modeling uncertainty propagation in physical applications; stochastic differential equations can be solved based on a truncated PC representation, employing Galerkin projections onto a finite subspace spanned by these polynomials as a way of simplifying the equations themselves [21].

The use of Hermite polynomials is particularly efficient when the input uncertainty is Gaussian-distributed, as that it can then be expressed through a first-order Hermite chaos expansion. An extension was proposed by Xiu and Karniadakis [22] to deal with more general random inputs more efficiently. The underlying concept remains the same but the Hermite polynomials basis is replaced by a generic basis of orthogonal polynomials. A random process $Y(\theta)$ can then be expressed as

$$Y(\theta) = c_0 I_0 + \sum_{i_1=1}^{\infty} c_{i_1} I_1(\xi_{i_1}(\theta)) + \sum_{i_1=1}^{\infty} \sum_{i_2=1}^{i_1} c_{i_1 i_2} I_2(\xi_{i_1}(\theta), \xi_{i_2}(\theta)) + \sum_{i_1=1}^{\infty} \sum_{i_2=1}^{i_1} \sum_{i_3=1}^{i_2} c_{i_1 i_2 i_3} I_3(\xi_{i_1}(\theta), \xi_{i_2}(\theta), \xi_{i_3}(\theta)) + \cdots \quad (1)$$

where $I_n(\xi_{i_1}(\theta), \ldots, \xi_{i_n}(\theta))$ represents the Wiener–Askey polynomial of order n in terms of the random vector $\boldsymbol{\xi} = (\xi_{i_1}, \ldots, \xi_{i_n})$.

In complex applications, a direct modification of the mathematical system of equations describing the problem is often far from straightforward. Le Maître et al. [23] developed a nonintrusive polynomial chaos (NIPC) alternative, where the different modes of the expansion can be reconstructed by projecting deterministic computations onto the PC basis:

$$\hat{c}_i = \frac{1}{\langle \Phi_i^2 \rangle} \int \mathrm{d}\xi_1 \cdots \int \mathrm{d}\xi_N Y(\boldsymbol{\xi}) \Phi_i(\boldsymbol{\xi}) W(\boldsymbol{\xi}) \quad (2)$$

where $W(\boldsymbol{\xi})$ is the weighting function corresponding to the PC basis Φ_i.

Despite the relatively extensive literature available on the application of intrusive and nonintrusive PC formulations, the authors are aware of only five works that make active use of this method in the design of more robust systems: Choi et al. [24] apply a nonintrusive PC approach in the design of a three-bar structure under uncertain Gaussian-distributed load and material properties and of a joined-wing model under uncertainty in the material properties. Molina-Cristobal et al. [25] use an intrusive approach in the robust design of a simple electrical circuit with Gaussian-distributed uncertainties for resistance, inductance and input voltage. Dodson and Parks [26] use a nonintrusive collocation method in the robust design of an airfoil with four control variables and two uncertain Gaussian-distributed parameters (leading-edge and trailing-edge thicknesses). Zhao et al. [27] employ a nonintrusive PC formulation in the robust optimization of a 2-D airfoil with uncertainty in the location of the boundary-layer transition (modeled with a uniform distribution). Ghisu et al. [28] use an adaptive NIPC formulation in the robust optimization of an airfoil in the presence of an ice accretion with uncertain location, obtaining improved iced performance while maintaining acceptable clean characteristics.

III. Integrated Optimization System

In previous work [5,6] the authors have presented the integrated optimization of the design-point performance of a core compression system for a three-spool gas turbine engine composed of an intermediate-pressure compressor (IPC) and a high-pressure compressor (HPC) linked by an S-shaped duct. The integrated design approach allows process-intrinsic constraints needed to facilitate the isolated design of the different modules to be eliminated and the optimal configuration for the overall core compression system to be sought, and the use of an intelligent search mechanism (design optimization) enables the available design space to be searched effectively, yielding consistent gains in overall system performance and a simultaneous reduction in development times, through automation.

A. Parameterization Scheme

The shape of each component's annulus was specified through the definition of mean line and area distributions: a fourth-order polynomial was used in the mean line definition, and a fifth-order polynomial was used to define the area distribution, in order to give greater flexibility in each stage flow function. C^1 continuity was imposed at each interface. As required by the analysis software, pressure ratios across each stage and stator exit angles were specified. For each blade row, the number of blades and axial chords were allowed to vary. Solidities and aspect ratios are easily calculated as a function of axial chord and blade stagger and number. Thickness-to-chord ratios and nondimensional tip clearances were kept fixed, as they involve structural, material, and manufacturing considerations that go beyond the scope of this work. The design space is summarized in Table 1. Some of these variables were then fixed to meet the requirements of the contiguous components, and lower and upper bounds were set to avoid clearly infeasible regions being searched.

Table 1 Design space definition

Variable type	Count[a]
Mean line	$2m + 2$
Area distribution	$3m + 2$
Stage pressure ratios	n
Stator mean line flow exit angles	n
Blade mean line chords	$2n$
Blade numbers	$2n$
Total	$5m + 6n + 4$

[a]Here, m represents the number of modules and n is the total number of stages.

B. Evaluation Tools

A proprietary code for mean line performance prediction is used for compressor analysis. Given geometry and operating point, the code estimates the performance in terms of efficiency and operating margin, both at design-point and offdesign conditions. At the design point, blade angles are calculated based on the prescribed design-point pressure ratio distribution and air angles by application of the continuity equation and of a number of empirical correlations for boundary-layer development, blade incidence and deviation. At offdesign conditions, the prescribed mass flow and rotational speed are used to calculate boundary-layer development, incidence and deviation, and then losses and efficiencies. A prediction for the surge margin (calculated as a function of the actual total pressure ratio and the pressure ratio at surge: $\mathrm{SM} = 100[(\mathrm{PR}_{\mathrm{surge}} - \mathrm{PR})/\mathrm{PR}]$) is also made based on a number of different correlations.

A shortage of experimental investigations of axisymmetric S-shaped ducts has led to a lack of practical rules for duct design and evaluation [29] and to the frequent use of conservative designs in gas turbine applications [30,31]. With the development of powerful computers and efficient flow solvers, the use of CFD directly in the design process can allow previously unexplored solutions to be evaluated and artificial constraints to be replaced by real physical limits, with potentially significant advantages in terms of whole system performance. In this work, the finite volume axisymmetric CFD solver developed by Ghisu [32] was therefore used to evaluate the performance of the duct.

The main barrier to the direct use of CFD in the preliminary design process is the still considerable computational time it requires when compared with the lower-fidelity techniques generally adopted in this phase of the process. To minimize the impact of the use of this higher-fidelity, higher-cost tool on the development time, a reduced-order model (ROM) based on a radial basis function approach was constructed using a number of representative CFD evaluations, selected by populating the design space via an LP-τ sequence [17]. The ROM could be then constructed offline in a parallel environment, with a minimal impact on the optimization time. The number of parameters used to describe the S-shaped duct geometry was limited to six to allow a reliable global response surface to be constructed; the remaining $5m + 6n - 2$ variables describe the two compressors. One thousand CFD runs were used to build the ROM, with a coefficient of determination in excess of 0.98. In this way the optimization process was not hampered by the time required for CFD evaluation of duct performance, and a good degree of evaluation accuracy was maintained due to the limited dimensionality of the duct's design space. In larger problems, a different approach would probably be preferable (online local response surfaces [33] or successive updates of an initial model [18] are possibilities). More information is available in [32].

C. Optimizer

The tabu search (TS) algorithm developed by Jaeggi et al. [34] was selected for this work. TS is a metaheuristic method designed to help a search negotiate difficult regions (e.g., escape from local minima or cross infeasible regions of the search space) by imposing restrictions [35]. The local search phase at its core is conducted with the Hooke and Jeeves (H&J) algorithm [36], with the best allowed move being made. The short-term memory records the last S visited points, which are tabu and thus cannot be revisited. The effect of the short-term memory is that the algorithm behaves like a normal hill-descending algorithm until it reaches a minimum, then it is forced to climb out of the hollow and explore further. Two other important characteristics of the TS algorithm are intensification and diversification. Intensification is associated with the medium-term memory, where the best M solutions located are stored. Diversification is associated with the long-term memory, which records the areas of the search space that have been explored by dividing it into a number of sectors and tallying how many times each sector has been visited. On diversification the search is restarted in an underexplored region of the design space. The extension to multiobjective problems is straightforward: the medium-term memory contains the set of

nondominated solutions found, and at every H&J step a move is selected randomly from among the set of nondominated new designs. The discarded designs are not lost, however: they are stored in the medium-term memory, if appropriate, and can then be selected during intensification.

TS has been found to be particularly effective in the solution of real-world optimization problems. Because of the local search algorithm at its core, it is able to efficiently navigate the complex, highly constrained search spaces that are typical of such problems, and the larger design changes made by evolutionary algorithms tend to generate large numbers of infeasible designs [37,38]. This strength of TS can, however, become a weakness in very large design spaces, as H&J search requires a number of evaluations per optimization step approximately equal to twice the number of design variables. Ghisu et al. [39] introduced an improvement based on Principal Components' Analysis of the approximation set. This allows the design-space parameterization to be rotated toward its most energetic directions (those most likely to lead to improved solutions) and the design-space dimensionality to be temporarily reduced. By eliminating the less important (and often more noisy) design variables, this scheme reduces the number of evaluations required and simultaneously improves the search effectiveness.

IV. Methodology

A. Uncertainty Quantification

1. Compressor Working Line

Compressor performance is generally expressed in nondimensional (or corrected) terms: the compressor characteristic reports pressure ratio and efficiency as a function of nondimensional mass flow for several values of constant nondimensional speed. Figure 1 shows the compressor characteristic of a generic core multistage compressor. The most important features are: the constant corrected speed lines (extending from choke to surge), with the last one almost parallel to the vertical axis because of the first stages' choking at high rotational speeds; the surge line, which represents the location of surge (or rotating stall at low rotational speeds) at different rotational speeds because of excessive flow separation due to the increased flow incidence on the blades at reduced mass flows; and the working line, which represents the locus of stable compressor operation at the different rotational speeds.

The determination of the working line for any of the engine components (generally known as engine matching) is typically an iterative process, as each component's operation is influenced by other engine components. The operation of a compressor is greatly influenced by the turbine mounted on the same shaft. For the core compression system of a three-spool gas turbine engine,

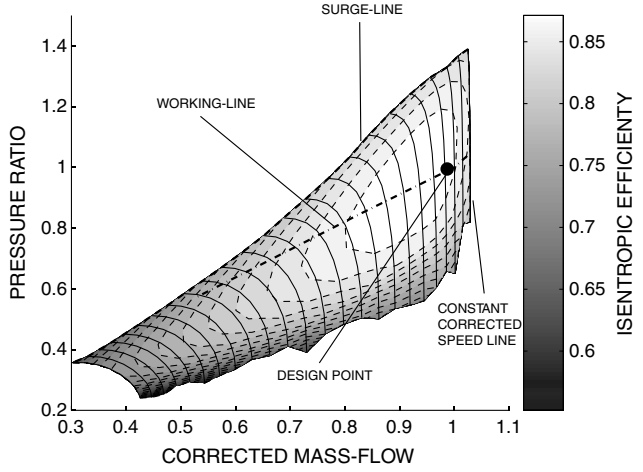

Fig. 1 Typical compressor characteristic: pressure ratio as a function of corrected mass flow is shown for several constant corrected speed lines together with isentropic efficiency contours.

$$\begin{cases} \mathrm{PR}_{\mathrm{IPC}} = \left(1 + k_1 \frac{T_{0,4}}{T_{0,2}} \eta_{\mathrm{LPC}}\right)^{\frac{\gamma}{\gamma-1}} \\ \bar{m}_{\mathrm{IPC}} = k_2 \mathrm{PR}_{\mathrm{IPC}} \mathrm{PR}_{\mathrm{HPC}} \sqrt{\frac{T_{0,2}}{T_{0,4}}} \\ \mathrm{PR}_{\mathrm{HPC}} = \left(1 + k_3 \frac{T_{0,4}}{T_{0,25}} \eta_{\mathrm{HPC}}\right)^{\frac{\gamma}{\gamma-1}} \\ \bar{m}_{\mathrm{HPC}} = k_4 \mathrm{PR}_{\mathrm{HPC}} \sqrt{\frac{T_{0,25}}{T_{0,4}}} \end{cases} \tag{3}$$

The numbered subscripts correspond to states at entry to/exit from the components shown schematically in Fig. 2. Several assumptions were made in deriving these results [3]: constant mass flow through the system, constant power offtake, choked turbines, constant turbine efficiencies, and constant nozzle area. An iterative solution process is required, since both pressure ratios and nondimensional mass flows are dependent on the compressors' isentropic efficiencies, which, in turn, are functions of pressure ratios and nondimensional mass flows. The operating point thus depends (for a given system) only on the ratio $T_{0,4}/T_{0,2}$ (a function of the fuel flow or engine throttle), which can be regarded as the control variable of the system.

2. Additional Uncertainties

A number of assumptions were made in calculating the compressors' working lines in Eqs. (3), such as constant mass flow through the system, constant power offtake, constant turbine efficiencies, and choked turbine nozzles. Any of these parameters can be considered as an additional operational uncertainty, with its own (known or unknown) range of variability and probability density function (PDF).

B. Uncertainty Propagation by Means of NIPC

In previous work [4], the authors used an NIPC formulation, in terms of a system of orthonormal polynomials constructed adaptively based on the given input PDFs, to propagate the input uncertainties through the system under consideration. A generic response Y can be expressed in terms of its chaos expansion as

$$Y(\xi_1, \ldots, \xi_N) = a_0 \Pi_0 + \sum_{i_1=1}^{N} a_{i_1} \Pi_1(\xi_{i_1}) + \sum_{i_1=1}^{N} \sum_{i_2=1}^{i_1} a_{i_1,i_2} \Pi_2(\xi_{i_1}, \xi_{i_2}) + \sum_{i_1=1}^{N} \sum_{i_2=1}^{i_1} \sum_{i_3=1}^{i_2} a_{i_1,i_2,i_3} \Pi_3(\xi_{i_1}, \xi_{i_2}, \xi_{i_3}) + \ldots \tag{4}$$

or, if term-based indexing is used,

$$Y(\xi_1, \ldots, \xi_N) = \sum_{i=0}^{\infty} y_i \Theta_i(\xi_1, \ldots, \xi_N) \tag{5}$$

where each of the Θ_i is a multivariate polynomial obtained as a product of the one-dimensional orthonormal polynomials, and $(\xi_1, \ldots, \xi_N)$ are the support random variables for the chaos expansion, which in the current approach are obtained through a normalization of the input random variables. The summation in Eq. (5) is truncated for practical purposes to a finite order p, giving a

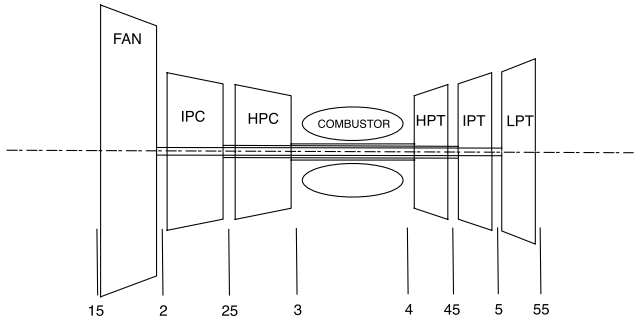

Fig. 2 Schematic of a three-spool gas turbine.

total of $(p+N)!/p!N!$ terms, where N is the number of random variables.

Each of the coefficients of the PC expansion can be obtained by projecting the generic variable onto the elements of the PC basis:

$$y_i = \int_{\Upsilon} Y(\boldsymbol{\xi})\Theta_i(\boldsymbol{\xi})W(\boldsymbol{\xi})\,\mathrm{d}\boldsymbol{\xi} \tag{6}$$

where Υ is the hypercube defining the random variables' space $[(0,1)^N$ in this case], and $W(\boldsymbol{\xi})$ is the joint PDF, corresponding to

$$\prod_{k=1}^{N} W(\xi_k)$$

under the assumption of independent random variables.

The integral in Eq. (6) can again be calculated through a quadrature approach. The simplest technique for calculating multidimensional integrals is a tensor product of the one-dimensional quadrature rules:

$$y_i = \frac{1}{\langle \Theta_i^2 \rangle} \sum_{n_1=1}^{N_0} \cdots \sum_{n_N=1}^{N_0} Y(\xi_{n_1}, \ldots, \xi_{n_N})\Theta_i(\xi_{n_1}, \ldots, \xi_{n_N}) \prod_{k=1}^{N} w_{n_k} \tag{7}$$

The use of the Gaussian abscissas (corresponding to the roots of the orthonormal polynomials) and weights is particularly convenient as it ensures an exact integration of polynomials of degree up to $2N_0 - 1$, where N_0 is the order of the quadrature formula.

A full tensor product quadrature formula is an effective approach for calculating multidimensional integrals when the number of dimensions is relatively small, but, since the number of collocation points grows exponentially with the number of random dimensions, its effectiveness deteriorates rapidly for larger dimensionality problems. In contrast, the convergence rate of MCS is only mildly dependent on the number of random uncertainties [40]. In practice, if a system is characterized by a large number of input uncertainties, the chances of these being interdependent are quite high: a Karhunen–Loève expansion can be used to decompose the input multidimensional noise in terms of its principal components and to isolate the most energetic sources of uncertainty, which can, in many cases, be limited to a relatively small number [21].

In problems with a moderately large number of variables, sparse tensor product grids (first proposed by Smolyak [41]) can be used to reduce the number of collocation points, while preserving a high level of accuracy. Nobile et al. [40] proved the effectiveness of sparse grid collocation approaches (when compared with MCS) for a stochastic linear elliptic problem in two spatial dimensions with up to 11 independent random variables.

An alternative approach is to use a least-squares estimation to calculate the coefficients of the PC expansion. Recalling that a generic functional Y can be approximated as a truncated PC expansion,

$$Y(\xi_1, \ldots, \xi_N) \approx \sum_{i=0}^{P} y_i \Theta_i(\xi_1, \ldots, \xi_N) \tag{8}$$

the coefficients can also be calculated by solving the following system:

$$\boldsymbol{\Theta}\mathbf{C} = \mathbf{Y} \tag{9}$$

where $\boldsymbol{\Theta}$ is an $N_t \times [(p+N)!/p!N!]$ matrix containing in each line the values of the $(p+N)!/p!N!$ orthogonal polynomials at each collocation point, $\mathbf{C}$ a vector containing the $(p+N)!/p!N!$ coefficients of the expansion, and $\mathbf{Y}$ a vector containing the values of the generic functional at the N_t collocation points. To avoid $\boldsymbol{\Theta}$ being poorly conditioned, N_t has to be larger than the number of unknowns. Different techniques exist for selecting the collocation points (random sampling, LP-τ sequences, and Latin hypercube techniques are common examples), but using a subset of the Gaussian quadrature points (those with the highest weight) as the collocation points represents a particularly efficient approach [42].

Given the functional relationship between the input uncertainties and the performance metrics of interest, the relevant statistics can be rapidly calculated. Only mean and variance are reported:

$$\mu = \int \cdots \int \sum_{i=0}^{p} y_i \Theta_i(\boldsymbol{\xi}) W(\boldsymbol{\xi})\,\mathrm{d}\boldsymbol{\xi} = y_0 \tag{10}$$

$$\sigma^2 = \int \cdots \int \left(\sum_{i=0}^{p} y_i \Theta_i(\boldsymbol{\xi}) - y_0 \right)^2 W(\boldsymbol{\xi})\,\mathrm{d}\boldsymbol{\xi} = \sum_{i=1}^{p} y_i^2 \tag{11}$$

V. Results

A. Design-Point Integrated Optimization

The design-point (DP) optimization of the system introduced in Sec. III sought to improve its overall efficiency without compromising the operating margins of the two compressors. In contrast to the traditional optimization approach, in which IPC, HPC, and intercompressor duct are largely designed (and optimized) in isolation by setting interface conditions (process-intrinsic constraints [43]), constraints here were set only at the IPC entry plane and HPC exit plane, leaving every other design parameter free during the optimization process. The use of a multiobjective approach allows the compromise between the conflicting objectives to be identified and a family of solutions with improved characteristics to emerge to the attention of the designer.

The resulting three-objective optimization problem is as follows:

$$\text{Maximize } \eta_{\text{tot}}, \quad \text{SM}_{\text{IPC}}, \quad \text{SM}_{\text{HPC}}$$

$$\begin{aligned} \text{Subject to } & \text{PR}_{\text{IPC}} = \overline{\text{PR}_{\text{IPC}}}, \quad \text{PR}_{\text{HPC}} = \overline{\text{PR}_{\text{HPC}}}, \quad \dot{m} = \bar{\dot{m}} \\ & \text{DH}_{\min} \geq \overline{\text{DH}}, \quad \text{SPR}_{\max} \leq \overline{\text{SPR}}, \quad \text{DF}_{\max} \leq \overline{\text{DF}} \\ & \text{Koch}_{\max} \leq \overline{\text{Koch}}, \quad H_{\substack{\max \\ \text{duct}}} \leq \bar{H} \end{aligned}$$

Overall system efficiency [derived with the assumption of adiabatic flow, as shown in Eq. (12)]:

$$\eta_{\text{tot}} = \frac{(\text{PR}_{\text{IPC}}\text{PR}_{\text{HPC}})^{\frac{\gamma-1}{\gamma}}(1-\omega)^{\frac{\gamma-1}{\gamma}} - 1}{\left(\frac{\text{PR}_{\text{IPC}}^{\frac{\gamma-1}{\gamma}}-1}{\eta_{\text{IPC}}}+1\right)\left(\frac{\text{PR}_{\text{HPC}}^{\frac{\gamma-1}{\gamma}}-1}{\eta_{\text{HPC}}}+1\right)-1} \tag{12}$$

and IPC and HPC surge margins are to be maximized simultaneously, subject to a number of inequality constraints that limit the level of loading carried by the different blade rows (through a number of common loading factor parameters, such as de Haller number DH, static-pressure-rise coefficient SPR, diffusion factor DF, and Koch factor). Mass flow and IPC and HPC pressure ratios were kept fixed at their original values, together with a number of variables (such as IPC inlet flow area, radius, and flow angle and HPC exit area, radius, and flow angle) to avoid subsequent changes to other components, which could have compromised the engine's performance. The maximum duct boundary-layer shape factor H was added as a further constraint, to avoid the occurrence of separated flows in the duct enabling higher-efficiency systems to be obtained at the price of flow instabilities that would be unacceptable for the performance of downstream components. The shape factor is a measure that can give some indication of how close a boundary layer is to separation. A review of some widely used criteria for separation is given by Castillo et al. [44]; these generally assume a value of H at separation between 2.4 and 2.8.

The Pareto front resulting from the three-objective optimization problem is presented in Fig. 3 (with performance being measured relative to that of a datum design). Consistent improvements in performance are possible: separate improvements of about 1.2 percentage points (PPs) in system efficiency or 10 and 8 PPs in IPC and HPC surge margins, respectively, can be achieved; alternatively, compromise designs with lower improvements in all three objectives could be chosen. A more detailed description of the system and of the optimization problem, together with a thorough analysis of the results, is presented elsewhere [5,6].

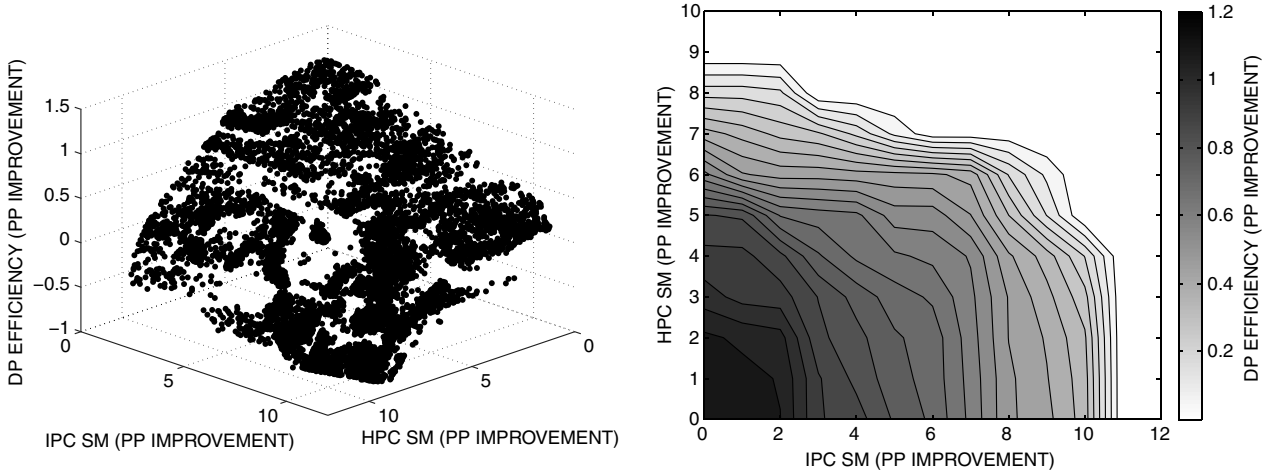

a) 3-D objective space **b) Contour plot of DP efficiency improvement**

Fig. 3 Results from the design-point integrated optimization of the core compression system [6].

B. Decision-Making by Means of Robust Analysis

The assumption of nominal values for uncertain parameters is a common simplification in the design of engineering systems, but the ability to attain improved performance in an idealized situation might not be sufficient to guarantee improved performance in real-world conditions. The tendency of heavily optimized designs to perform poorly in offdesign conditions is well documented [1]. For a proposed new design to be considered a real improvement over a datum design, its sensitivity in the face of likely uncertainties must be evaluated. The NIPC approach presented in Sec. IV.B represents a relatively inexpensive method (compared with MCS) for propagating a number of stochastic inputs through a generic system, without needing to modify the analysis tools in use.

This approach has been used to analyze the variability in performance in the face of a number of operational uncertainties of the designs obtained through the design-point optimization (Sec. V.A). In addition to the engine throttle (the importance of which in determining a compressor's operating point has been highlighted in Sec. IV.A.1), power offtake and air bleed were also considered as random variables with given PDFs. Assuming a fraction of the inlet mass flow to be extracted at the IPC exit and a power offtake from the HPC, Eqs. (3) can be modified as follows:

$$\begin{cases} \mathrm{PR}_{\mathrm{IPC}} = \left(1 + k_1 \frac{\tau_1}{\tau_2} \eta_{\mathrm{LPC}}\right)^{\frac{\gamma}{\gamma-1}} \\ \bar{m}_{\mathrm{IPC}} = k_2 \mathrm{PR}_{\mathrm{IPC}} \mathrm{PR}_{\mathrm{HPC}} \frac{\tau_2}{\sqrt{\tau_1}} \\ \mathrm{PR}_{\mathrm{HPC}} = \left(1 + k_3 \frac{\tau_1}{\tau_3} \frac{T_{0,2}}{T_{0,25}} \eta_{\mathrm{HPC}}\right)^{\frac{\gamma}{\gamma-1}} \\ \bar{m}_{\mathrm{HPC}} = k_4 \mathrm{PR}_{\mathrm{HPC}} \sqrt{\frac{T_{0,25}}{T_{0,2}}} \frac{1}{\tau_1} \end{cases} \tag{13}$$

where $\tau_1 = T_{0,4}/T_{0,2}$, $\tau_2 = \dot{m}_{\mathrm{IPC}}/\dot{m}_{\mathrm{HPC}}$ is the ratio of the mass flows before and after the air bleed, and

$$\tau_3 = \frac{\dot{W}_{\mathrm{HPT}}}{\dot{W}_{\mathrm{HPC}}} = 1 + \frac{\dot{W}_{\mathrm{OT}}}{\dot{W}_{\mathrm{HPC}}}$$

is the ratio between high-pressure turbine work and high-pressure compressor work, a function of the power offtake $\dot{W}_{\mathrm{OT}}$.

The PDFs shown in Fig. 4 were assumed for the three uncertain parameters τ_1, τ_2 and τ_3. They do not represent any particular standard distributions (i.e., they are nonstandard PDFs) and they were chosen to demonstrate the generality of this approach. The bimodal PDF for the engine throttle was chosen in light of the importance of two particular operating conditions (maximum power and cruise). Any alternative PDFs could be used instead, without requiring any modifications to the approach presented here. The three input PDFs are noncorrelated, for simplicity. If this had not been the case, the input distributions could have been expressed in terms of noncorrelated random variables through a Karhunen–Loève expansion, as shown by Ghanem and Spanos [21].

The designs in the Pareto front obtained from the design-point optimization presented in Sec. V.A were analyzed using the proposed approach for uncertainty propagation. The results are shown in Fig. 5a, in which the design-point system isentropic efficiency has been replaced by the mean isentropic efficiency obtained in the face of the operational uncertainties specified. It is clear that the improvement in mean performance is substantially less than the improvement in design-point performance, shown in Fig. 3. Figure 5b reports only the nondominated designs in terms of the new performance metrics (mean system efficiency and IPC and HPC surge margins) from among those analyzed: only about 12% of the original designs are now nondominated, demonstrating the value of robust analysis in

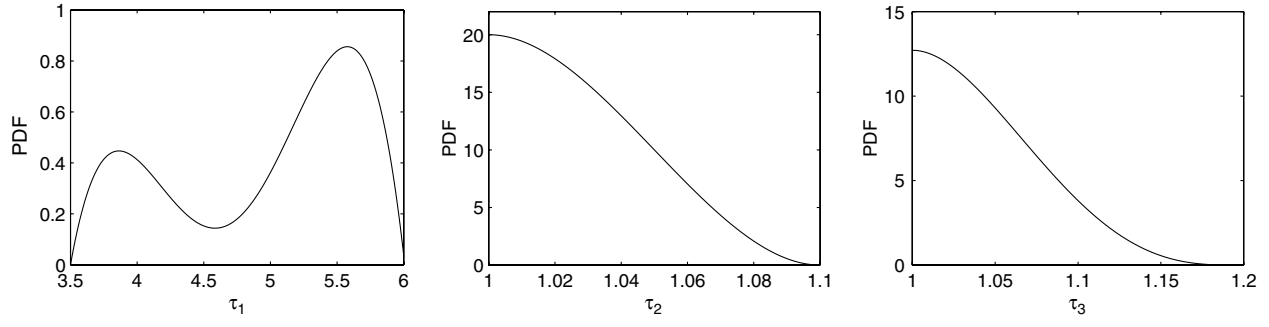

Fig. 4 PDFs for the input uncertainties; left: τ_1 (engine throttle), middle: τ_2 (air bleed), and right: τ_3 (power offtake).

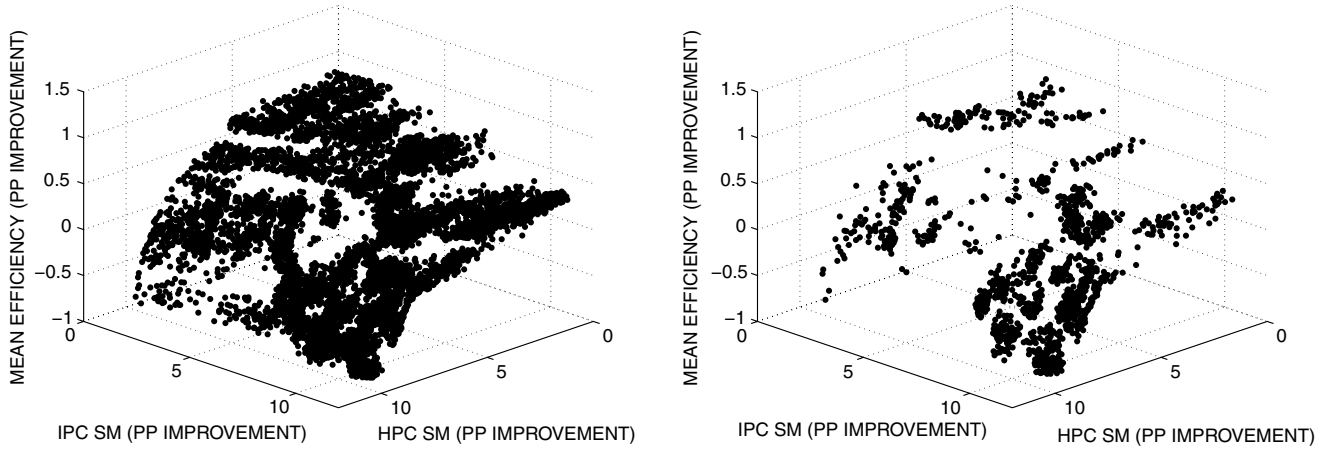

a) Every Pareto front design **b) Nondominated designs**

Fig. 5 Robust analysis of the Pareto front obtained by traditional (DP) optimization, with mean isentropic efficiency replacing DP isentropic efficiency as one of the objectives.

identifying designs that are less sensitive to the presence of given uncertainties in design or operational parameters.

Figure 6 shows a comparison between the maximum and minimum improvements in mean system efficiency, as a function of IPC and HPC SM improvements, that can be achieved with the design configurations identified by the design-point optimization. The difference between the two contour plots represents the performance penalty that can result from a poor choice of design solution, in the absence of any robust analysis. The variability in mean performance for a similar combination of IPC and HPC surge margins suggests that better (from a mean performance perspective) designs should be obtained by successfully integrating the robust analysis within the optimization process.

More important than the improvement in some figures of merit is the safe operation of the given designs. In compression systems, this means that the operating point must be at a sufficient distance from the occurrence of stall, at all throttle settings. Although adequate design-point surge margins for both IPC and HPC were ensured by treating these two metrics as design objectives, there is no guarantee that the same will also apply to different operating conditions, especially at low throttle settings, where working line and surge line tend to converge, especially for large-pressure-ratio compressors [3]. Figure 7 shows only the nondominated designs with a minimum surge margin not lower than the minimum surge margin of the datum design, both as a three-dimensional plot (Fig. 7a) and as a contour plot (Fig. 7b). It is again clear that the gains in mean performance are less than the design-point efficiency gains shown in Fig. 3b.

Figure 8 presents a comparison between the maximum design-point isentropic efficiency configuration, design A, and the maximum mean efficiency safe design (with a satisfactory minimum surge margin at every operating condition), design B, identified after the decision-making process guided by the robust analysis. Figure 8b presents a close-up view of the intercompressor duct.

Figure 9 compares the IPC characteristics for the two configurations, together with the PDFs for the position of the operating point. The most noticeable difference is the increased part-speed surge margin of design B (the working area of the maximum DP efficiency configuration reaches the surge line at lower rotational speed). Figure 10 presents the same comparison for the two HPCs. The working area is smaller than that of the IPCs, as can be deduced from Eq. (13); low-pressure turbomachines generally have wider operating ranges than high-pressure turbomachines.

Figure 11 presents a comparison between the PDFs for the system isentropic efficiencies (Fig. 11a) and for IPC and HPC efficiencies (Figs. 11b and 11c), respectively. Design B has a lower variability in performance (the standard deviation is reduced by 0.7 PPs), but also lower mean performance (0.26 PPs lower than that of the maximum DP efficiency configuration). Crucially, design B's operating point maintains a sufficient margin from the occurrence of stall at every operating condition, but at the price of a slightly reduced mean

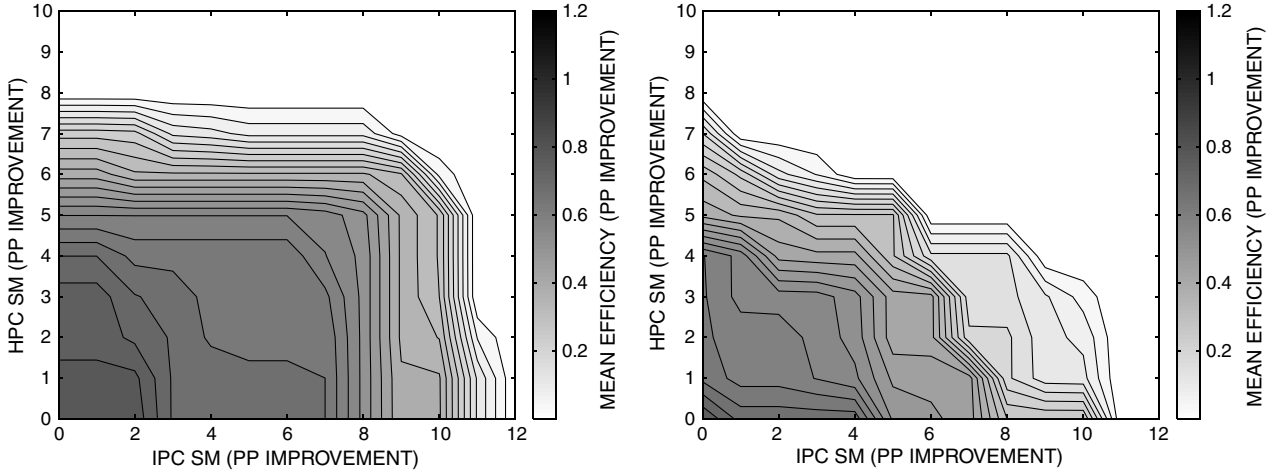

a) Best designs **b) Worst designs**

Fig. 6 Comparison between maximum and minimum improvements in mean isentropic efficiency achievable by the designs obtained through the DP optimization, as a function of IPC and HPC surge margins.

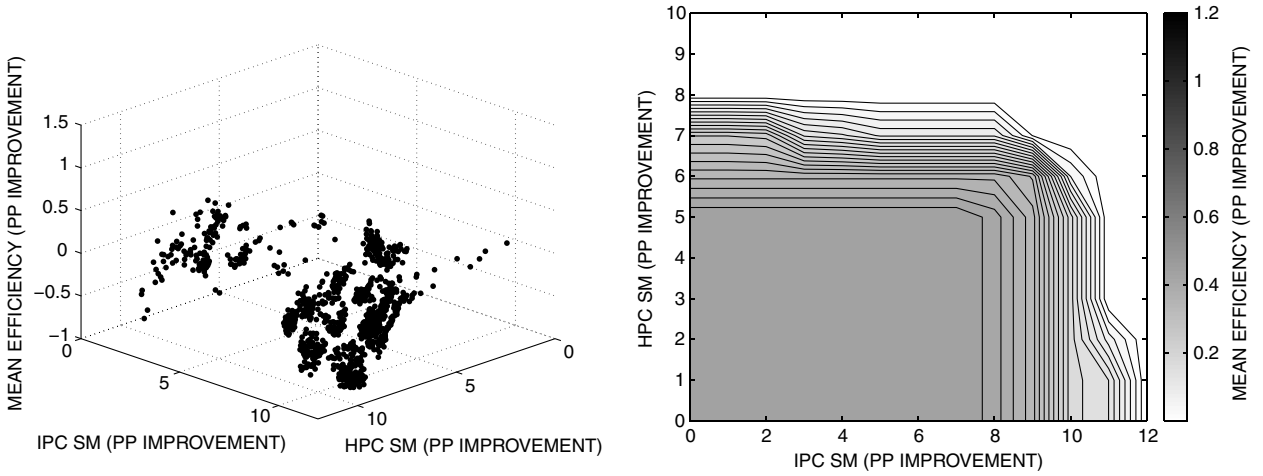

a) 3-D objective space **b) Contour plot**

Fig. 7 Feasible designs (with a safe minimum surge margin at every operating condition).

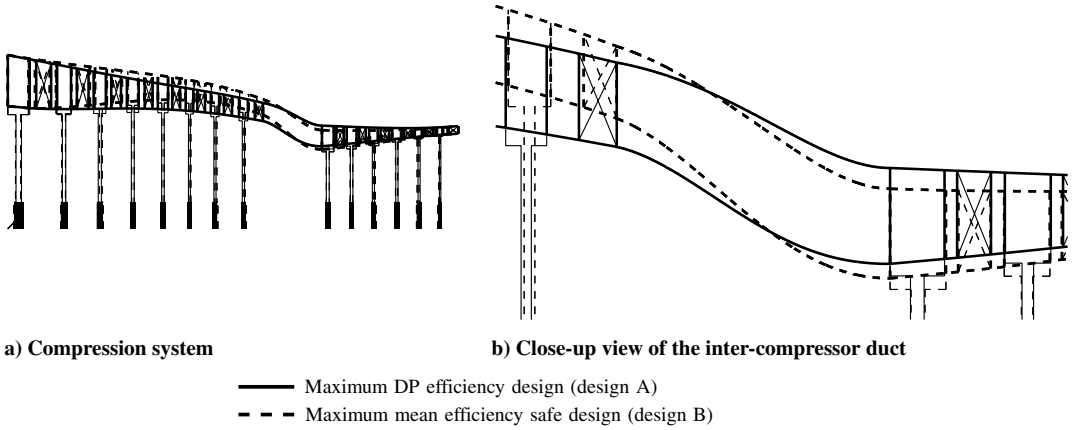

a) Compression system **b) Close-up view of the inter-compressor duct**

Maximum DP efficiency design (design A)
Maximum mean efficiency safe design (design B)

Fig. 8 Comparison between maximum DP efficiency and maximum mean efficiency compression systems.

performance. The lower probability of the compression system working at low efficiency is entirely due to the change in the IPC's performance PDF (the minimum IPC isentropic efficiency has been increased by 1.24 PPs, whereas the maximum value has only dropped by 0.16 PPs). Interestingly, the HPC's performances have been negatively affected, with a mean performance reduction of 0.8 PPs, due essentially to a shift of the PDFs toward lower efficiencies. The IPC has a larger impact on the mean performance because of its higher design pressure ratio (and lower inlet temperature), with the consequent effect on system efficiency as calculated through Eq. (12).

Figures 12 and 13 present a comparison between the compressor and efficiency characteristics for the two configurations, for IPC and HPC, respectively. Although there is an evident deterioration in IPC peak efficiency, which is present even at reduced rotational speeds, the compressor is used with higher probability close to the peaks of the efficiency curves, with a consequent improvement in performance and an increase in the surge margin, at every operating

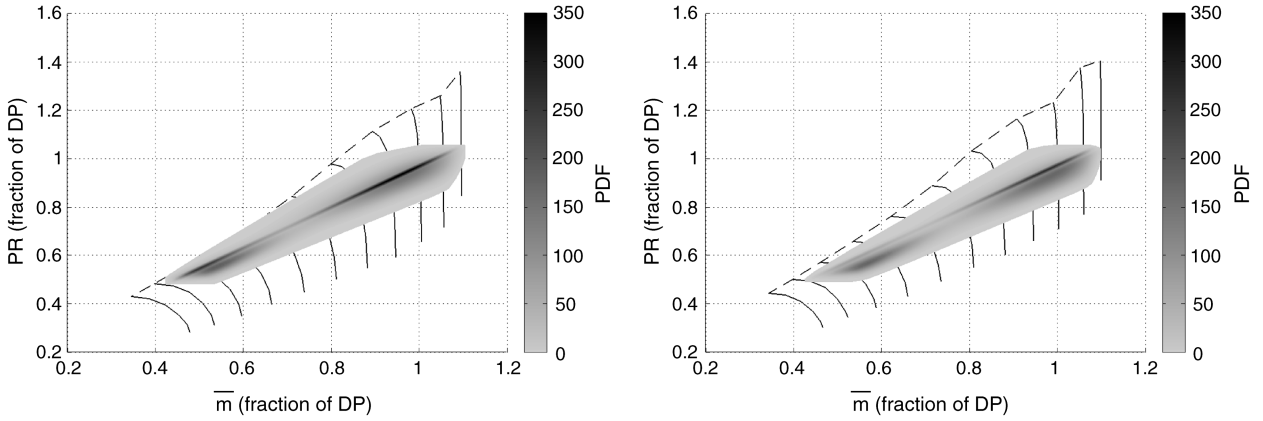

a) Maximum DP efficiency design **b) Maximum mean efficiency design**

Fig. 9 IPC characteristics with operating point PDFs.

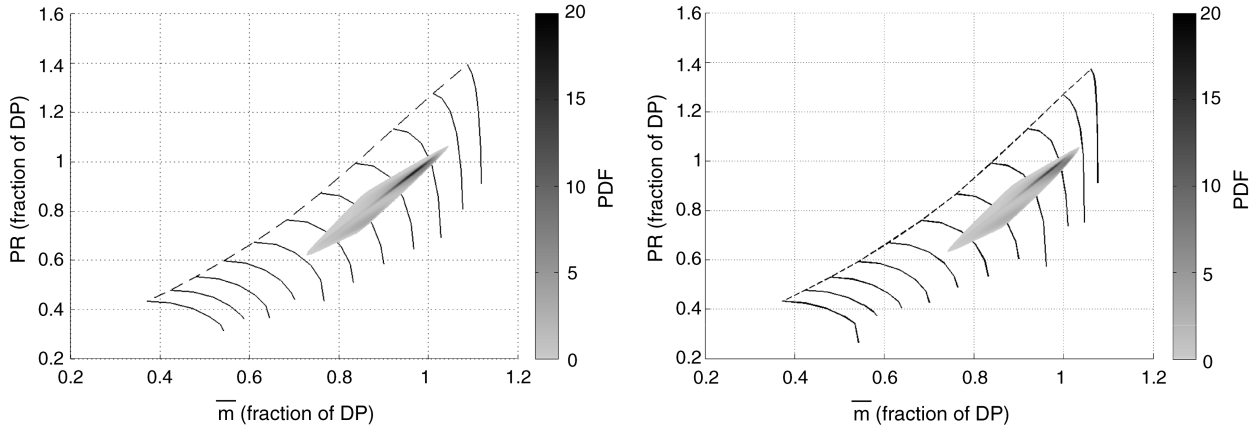

a) Maximum DP efficiency design b) Maximum mean efficiency design

Fig. 10 HPC characteristics with operating point PDFs.

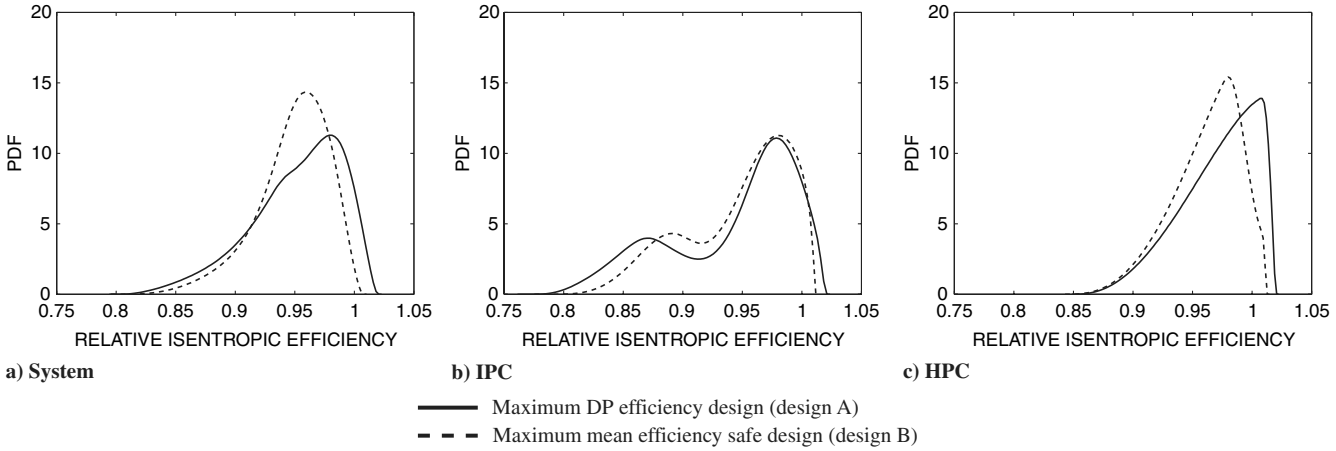

a) System b) IPC c) HPC

Fig. 11 Isentropic efficiency PDFs: comparison between maximum DP efficiency design and maximum mean efficiency safe design.

condition. The performance of the HPC is also penalized, especially at high nondimensional rotational speeds, but it must be noted that the impact on the overall system performance is minimal as the HPC operating range is smaller than that of the IPC (Fig. 10).

Apart from being linked in terms of offdesign behavior through Eq. (13), IPC and HPC are also physically connected through the intercompressor duct. Ghisu et al. [5,6] demonstrated the importance of an integrated approach to the design and optimization of gas turbine engines, in order to fully exploit the performance capabilities of the overall system. For this reason, the interfaces between the different subsystems were allowed to change freely, with the only constraint being the requirement to retain a duct with a sufficient margin from the occurrence of flow separation. Design B's duct has a $\Delta R/L$ (ratio of radial offset to length) 36% larger than design A, with

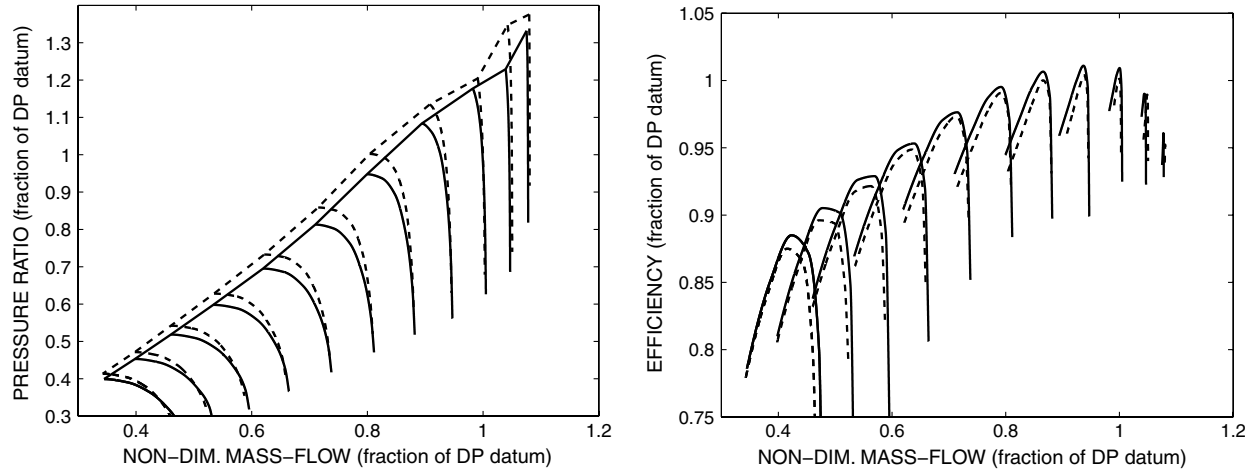

a) Pressure ratio/non-dimensionalized mass-flow b) Efficiency/non-dimensionalized mass-flow

Fig. 12 IPC characteristics comparison.

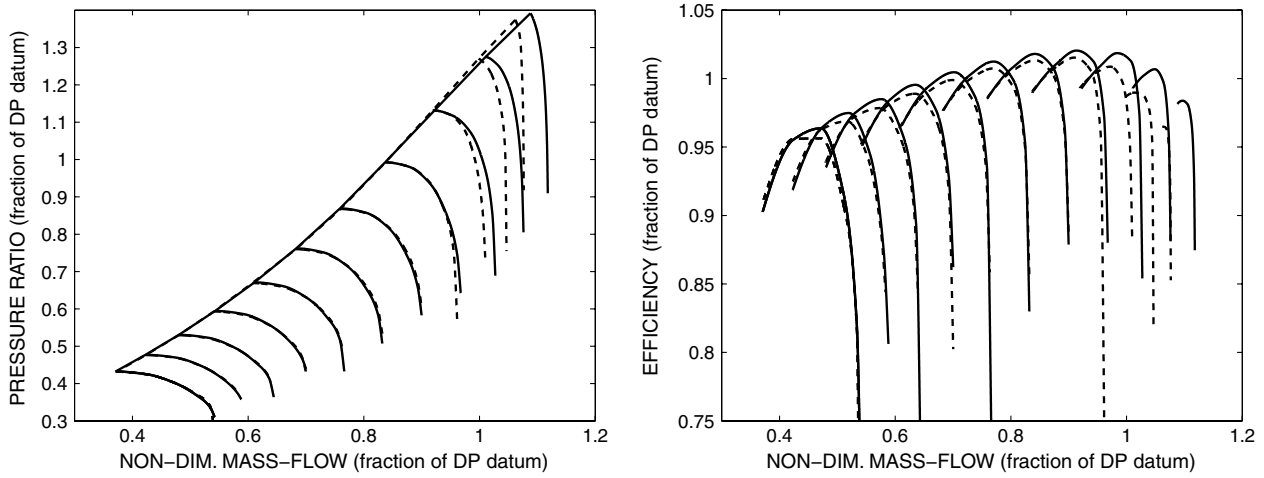

Fig. 13 HPC characteristics comparison.

a similar area ratio (0.5% less accelerating), but with a reduction in both inlet (10.9%) and exit (10.5%) area. The maximum DP efficiency configuration (design A) features a duct with a loading well within the acceptable limits (as shown elsewhere by the authors [6,45]). Design B presents a duct with a higher loading, but still with a sufficient margin from the occurrence of flow separation. The wall boundary-layer shape factors for the two ducts are compared in Fig. 14. The design B duct also has a larger loss coefficient[¶] (+28.5%) and a larger overall pressure loss (+68%), due to the larger flow velocity. The lower-performing duct is acceptable, however, in light of the improved overall performance of the compression system.

It is interesting to note that although the reduction in the peak performance of the IPC has allowed an improvement in its part-speed performance, design B's HPC presents a worse performance than the design A HPC at all operating conditions. Combining the design A IPC and the design B HPC is impossible, however, since the corresponding duct (with a lower $\Delta R/L$ but a higher area ratio than the design B duct) would be excessively loaded (too high of a maximum shape factor).

Robust analysis of the results from a design-point optimization has allowed the identification of a number of solutions with satisfactory behavior in the presence of the given PDFs for the input parameters. The use of an integrated design approach, with the associated increase in the available design space, was crucial to the success of the process: design B obtains an improvement in IPC performance (larger part-speed surge margin and lower variability in efficiency) at the cost of deteriorations in the performance of duct and HPC, but with better overall system performance as a result.

C. Robust Optimization

In the previous section, the results from the design-point optimization of the core compression system were analyzed using the NIPC approach to determine their sensitivity relative to a number of uncertain parameters. This approach allowed designs with satisfactory offdesign behavior (both in terms of part-load performance and operating margins) to be identified and those that did not meet these requirements to be discarded. This robust analysis approach was then integrated within the optimization loop to seek further improvements in mean performance (i.e., even more robust designs). To further reduce the computational requirements, the optimization was initialized with the designs obtained from the robust analysis of the design-point optimization results.

[¶]Ratio between stagnation pressure loss and inlet dynamic head.

Higher moments (e.g., variance) were not considered in the optimization, for two reasons. First is the consideration of the greater importance of mean performance for this particular problem (the objective is to minimize the total amount of fuel used, not how well it is used at the different operating points, provided that safety requirements are met). Second, the significant reduction in mean performance compared with the design-point performance was caused by a deterioration in offdesign performance: if designs with an improved mean efficiency exist, they will intrinsically have reduced performance variability compared with those obtained with the design-point optimization approach. The robust optimization problem tackled is as follows:

$$\text{Maximize } \mu_{\eta_{\text{tot}}}, \quad \text{SM}_{\text{IPC}}, \quad \text{SM}_{\text{HPC}}\varrho$$

$$\text{Subject to } \text{PR}_{\text{IPC}} = \overline{\text{PR}_{\text{IPC}}}, \quad \text{PR}_{\text{HPC}} = \overline{\text{PR}_{\text{HPC}}}, \quad \dot{m} = \bar{\dot{m}},$$
$$\text{DH}_{\min} \geq \overline{\text{DH}}, \quad \text{SPR}_{\max} \leq \overline{\text{SPR}}, \quad \text{DF}_{\max} \leq \overline{\text{DF}},$$
$$\text{Koch}_{\max} \leq \overline{\text{Koch}}, \quad H_{\max_{\text{duct}}} \leq \bar{H}, \quad \text{SM}_{\text{IPC,min}} \geq \overline{\text{SM}}_{\text{IPC,min}},$$
$$\text{SM}_{\text{HPC,min}} \geq \overline{\text{SM}}_{\text{HPC,min}}$$

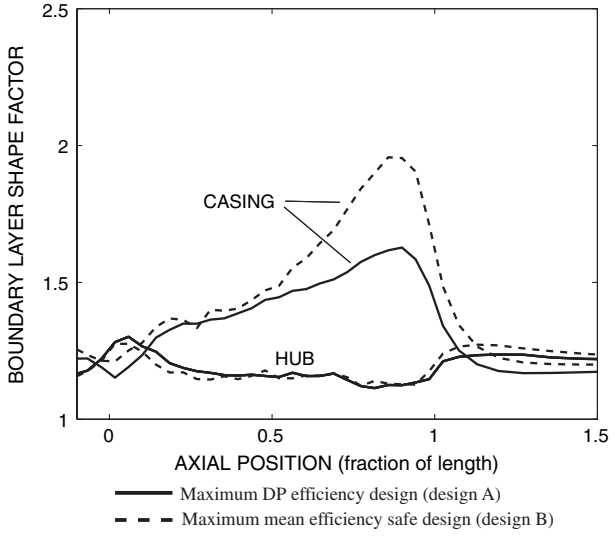

Fig. 14 Comparison of ducts' boundary-layer shape factors.

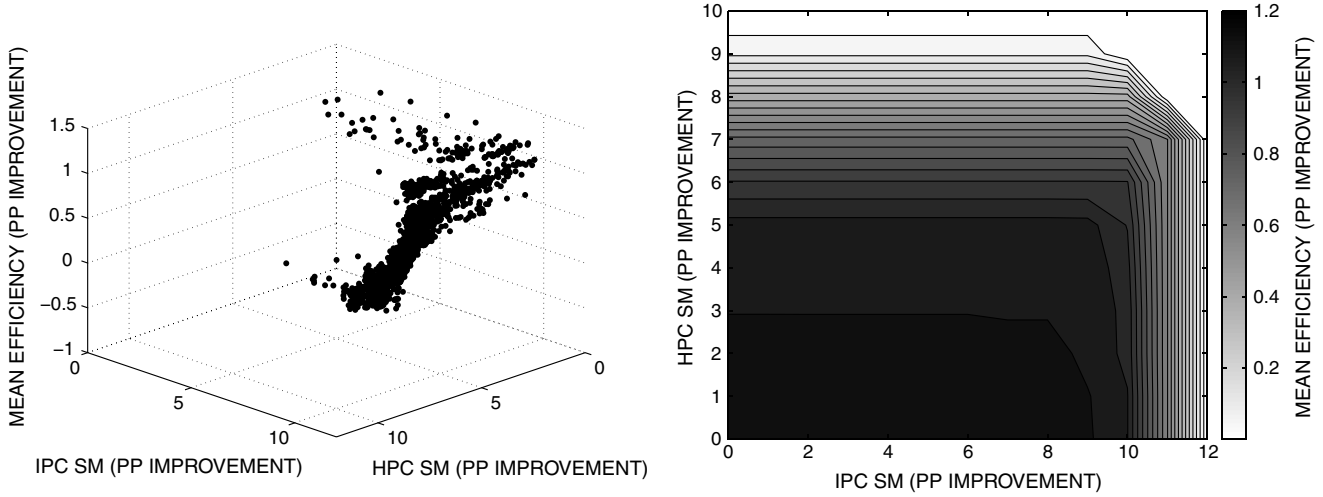

a) 3-D objective space **b) Contour plot**

Fig. 15 Results from the robust optimization of the core compression system.

Figure 15 presents the results from this robust optimization, again both as a three-dimensional plot of the improvements in the three figures of merit (Fig. 15a) and as a contour plot of the improvement in mean efficiency relative to combinations of improvements in IPC and HPC surge margins (Fig. 15b). The improvements in mean efficiency compared with those of the configurations obtained through robust analysis of design-point optimization solutions (Fig. 7b) are evident.

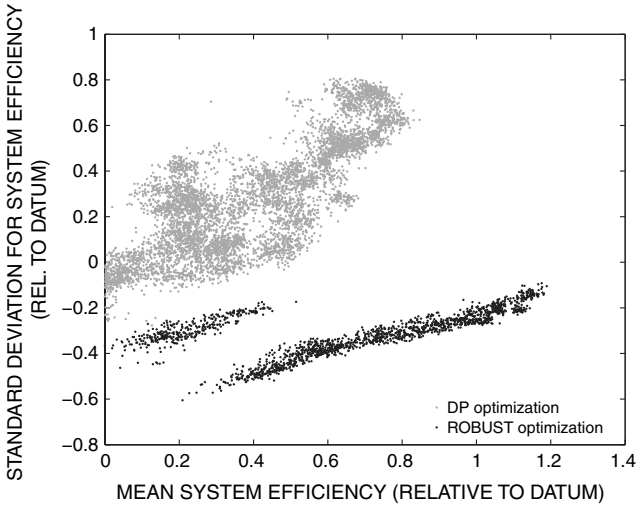

Fig. 16 Mean and standard deviation of system isentropic efficiency for the results of DP and robust optimizations.

Figure 16 presents a comparison of the results from the design-point and robust optimizations from the point of view of the mean value and standard deviation of system isentropic efficiency. As anticipated in the discussion above, not only is the mean improved by robust optimization, but the associated standard deviation is also reduced.

Figure 17 compares the maximum mean efficiency configuration obtained after robust analysis of the results of the DP optimization (design B) with the maximum mean efficiency configuration obtained from the robust optimization (design C); Fig. 17b presents a close-up view of the intercompressor ducts. Hub and casing profiles only differ slightly between the designs (the IPC's exit radius and HPC's inlet radius have been increased by 1.5 and 1.8%, respectively), and larger changes have been made to other design variables. All 94 design variables assume different values for the two designs, with 61 of them having a difference of more than 5% of the corresponding design variable range. The 10 variables with the largest differences are summarized in Table 2. Design C's intercompressor duct has similar $\Delta R/L$ (0.7% less than design B) and area ratio (+0.8%) values, with comparable maximum shape factor and pressure loss coefficient (the actual stagnation pressure loss is reduced by 3.6% due to a larger inlet flow area).

Figure 18 presents a comparison between the PDFs for the system isentropic efficiencies (Fig. 18a) and for IPC and HPC efficiencies

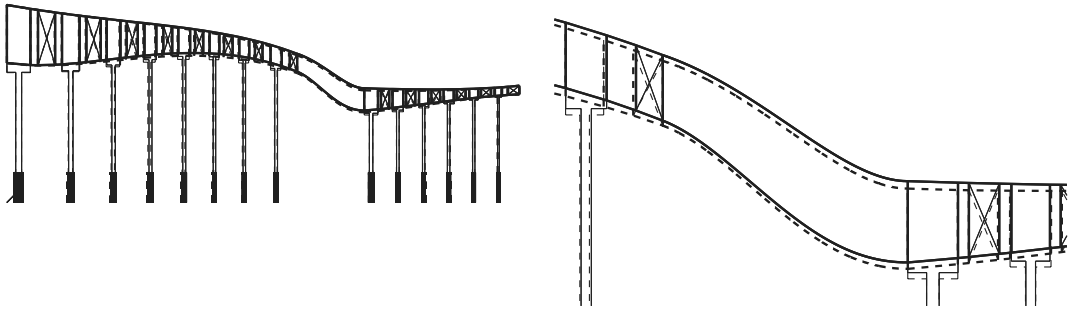

a) Compression system **b) Close-up view of the inter-compressor duct**

Robust Optimization (design C)
Traditional optimization followed by robust analysis (design B)

Fig. 17 Comparison between maximum mean efficiency designs after robust analysis and after robust optimization.

Table 2 Main differences between design B and design C

Design variable	Physical meaning	Difference (C–B, % of range)
42	Number of blades in IPC rotor 5	55
32	Exit flow angle after IPC stator 2	35
41	Number of blades in IPC rotor 4	34
93	Number of blades in HPC stator 5	30
36	Exit flow angle after IPC stator 6	28
51	Number of blades in IPC stator 6	25
82	Exit flow angle after HPC stator 5	24
49	Number of blades in IPC stator 4	24
37	Exit flow angle after IPC stator 7	24
65	Blade chord for HPC rotor 4	23

(Figs. 18b and 18c , respectively). Mean and standard deviation of system efficiency are both improved (by 0.75 and 0.21 PPs relative to design B, and 0.49 and 0.91 PPs relative to design A). The improvement in overall performance is due mainly to the improvement in the part-speed behavior of the IPC (see Figs. 18b and 19b). The minimum IPC efficiency has been increased by 2.3 PPs. HPC performance has also been improved slightly (see Figs. 18c and 20b).

VI. Conclusions

A common simplification in the engineering design process is to consider nominal values for a number of design parameters. Although making complex problems tractable, this approach can lead to products that present considerable performance degradation in real-world conditions. In gas turbine design, the different engine modules are usually designed with some specific operating condition in mind. The design point normally represents the most important operating condition (the one at which the engine spends the most time), but safe and satisfactory operation must be guaranteed at a number of other important points inside the engine performance envelope. In the traditional design approach, offdesign operation is usually considered only at a later stage of the design process. Although guaranteeing that minimum requirements are met, this approach risks the introduction of a further loop into the design process and, more

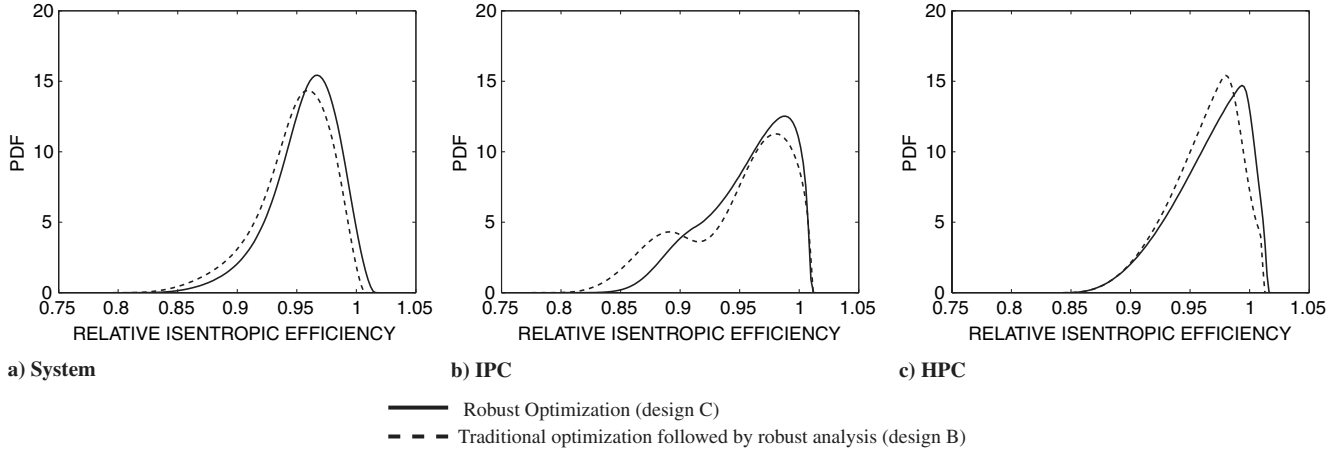

Fig. 18 Isentropic efficiency PDFs: comparison between maximum mean efficiency design after robust analysis and after robust optimization.

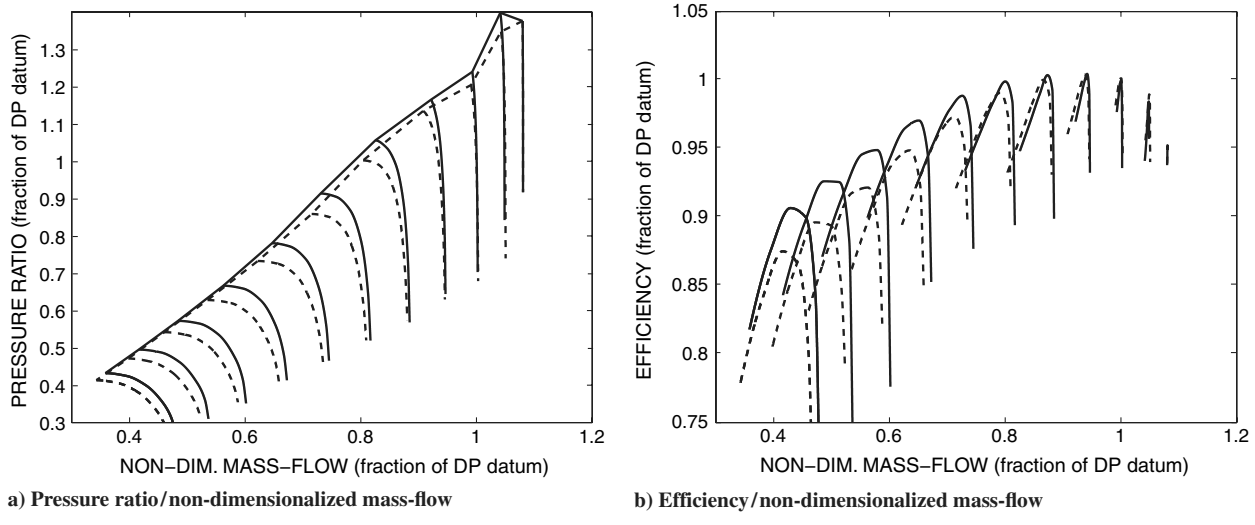

Fig. 19 IPC characteristics comparison.

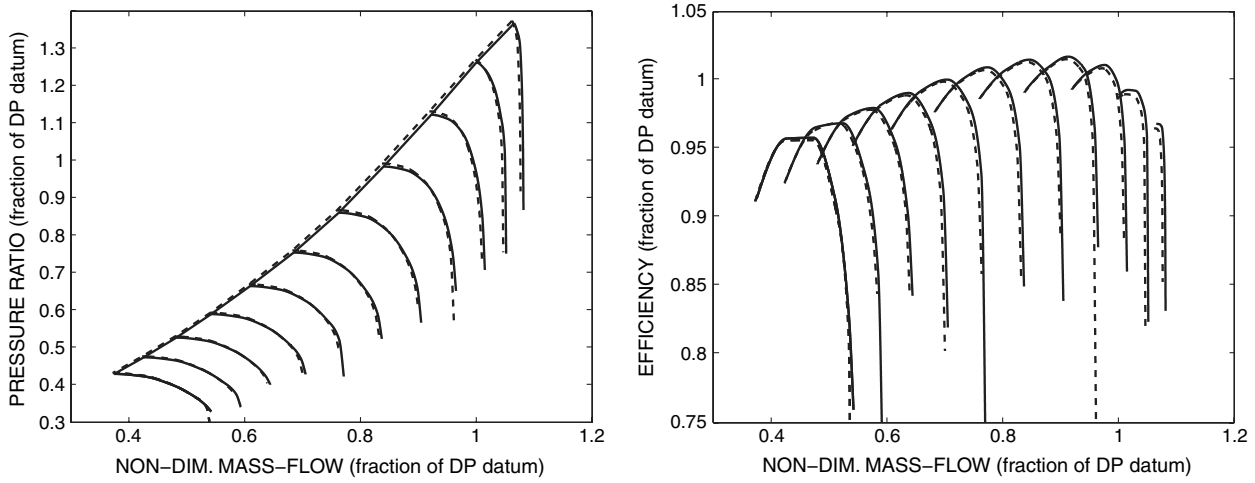

a) Pressure ratio/non-dimensionalized mass-flow **b) Efficiency/non-dimensionalized mass-flow**

Fig. 20 HPC characteristics comparison.

important, can lead to a product with suboptimal design-point and offdesign performance. Actively introducing some consideration of robustness into the design process can potentially produce significant improvements in real-world product performance.

In recent years, polynomial chaos has emerged as a reliable and relatively inexpensive technique (compared with Monte Carlo simulations) for uncertainty propagation. In its nonintrusive formulation, it allows the stochastic response of generic systems to be calculated as a combination of deterministic evaluations at specific values for the uncertain parameters. In previous work [4], a nonintrusive polynomial chaos approach, based on a set of orthonormal polynomials calculated in real time relative to the given uncertainty distributions, was employed to analyze the stochastic response of a core compression system from a three-spool gas turbine engine subject to uncertain operating conditions. The computational cost of the method, orders of magnitude less expensive than MCS (for a limited number of uncertain variables), facilitates its integration into the design process, with the potential of improving the real-world performance of engine systems and subsystems.

The method relies on the availability of detailed information for the input uncertainties. Even in the presence of uncertain PDF estimations, the use of a robust design approach can be beneficial: the result of a robust design process is a number of solutions with satisfactory performance over a range of operating conditions (and hence with more robust behavior than the design-point solutions, regardless of the specific PDFs used). A different set of input PDFs would almost certainly lead to a different family of robust solutions; however, the robust solutions found in the presence of given uncertainties would still be a better choice than the results of a traditional design optimization. Indeed, in the absence of any information about the input PDFs, a stochastic method for uncertainty analysis (such as PC or MCS) is probably not the most appropriate choice: alternative methods (sensitivity derivatives or interval analysis) can give an idea of the range of variability of the performance parameters and support the robust design process more effectively in these circumstances. Further information on alternative robust analysis methodologies can be found in [46].

In the present work, this approach was first used to analyze the stochastic response of designs resulting from a design-point optimization of the aforementioned core compression system in the presence of three uncertain parameters (representing engine throttle, air bleed and power offtake). This analysis allowed the design configurations with satisfactory offdesign performance (in the face of the specified uncertainties) to be identified and the excessively sensitive designs to be discarded. Variable stator vanes were not considered because of the relatively low overall pressure ratio of the intermediate-pressure compressor and because of the deterministic nature of their scheduling, but could be included without requiring modification to the approach used for uncertainty propagation.

The robust analysis method was then integrated within the optimization loop to seek further improvements in the overall performance of the system. Three maximum efficiency designs (one straight from the design-point optimization, one identified after the robust analysis of the design-point optimization results, and one from the robust optimization) were compared in detail, demonstrating how, in the presence of given uncertainties, better designs can be obtained through improvements in the offdesign behavior of the system rather than in its design-point performance. The results evidence the benefits of integrating robust analysis within the design optimization process, and demonstrate that the nonintrusive polynomial chaos approach offers a computationally affordable means of doing so. The results also provide further evidence of the benefits of a more integrated design process, since the same improvements in performance would not have been achievable through individual optimization of the separate modules.

References

[1] Keane, A. J., and Nair, P. B., *Computational Approaches for Aerospace Design*, Wiley, New York, 2005.

[2] Jeschke, P., Kurzke, J., Shaber, R., and Riegler, C., "Preliminary Gas Turbine Design Using the Multidisciplinary Design System MOPEDS," *Journal of Engineering for Gas Turbines and Power*, Vol. 126, No. 2, April 2004, pp. 258–264. doi:10.1115/1.1639009

[3] Cumpsty, N. A., *Jet Propulsion*, Cambridge Univ. Press, Cambridge, England, U.K., 1997.

[4] Ghisu, T., Parks, G. T., Jarrett, J. P., and Clarkson, P. J., "Adaptive Polynomial Chaos for Gas Turbine Compression Systems Performance Analysis," *AIAA Journal*, Vol. 48, No. 6, 2010, pp. 1156–1170. doi:10.2514/1.J050012

[5] Ghisu, T., Parks, G. T., Jarrett, J. P., and Clarkson, P. J., "An Integrated System for the Aerodynamic Design of Compression Systems—Part I: Development," *Journal of Turbomachinery*, Vol. 133, No. 1, 2011, Paper 011011. doi:10.1115/1.4000534

[6] Ghisu, T., Parks, G. T., Jarrett, J. P., and Clarkson, P. J., "An Integrated System for the Aerodynamic Design of Compression Systems—Part II: Application," *Journal of Turbomachinery*, Vol. 133, No. 1, 2011, Paper 011012. doi:10.1115/1.4000535

[7] Huyse, L., Padula, S. L., Lewis, R. M., and Li, W., "Probabilistic Approach to Free-Form Airfoil Shape Optimization Under Uncertainty," *AIAA Journal*, Vol. 40, No. 9, 2002, pp. 1764–1772. doi:10.2514/2.1881

[8] Putko, M. M., Newman, P. A., Taylor, A. C., and Green, L. L., "Approach for Uncertainty Propagation and Robust Design in CFD Using Sensitivity Derivatives," AIAA Paper 2001-2528, 2001.

[9] Taylor, A. C., Green, L. L., Newman, P. A., and Putko, M. M., "Some Advanced Concepts in Discrete Aerodynamic Sensitivity Analysis," AIAA Paper_2001-2529, 2001.

[10] Putko, M. M., Newman, P. A., and Taylor, A. C., "Employing Sensitivity Derivatives for Robust Optimisation Under Uncertainties in CFD," *9th ASCE Speciality Conference on Probabilistic Mechanics and Structural Reliability*, 2004.

[11] Gumbert, C. R., Newman, P. A., and Hou, G. J. W., "Effect of Random Geometric Uncertainty on the Computational Design of a Flexible Wing," AIAA Paper 2002-2806, 2002.

[12] Poloni, C., Pediroda, V., and Clarich, A., "A Fast and Robust Adaptive Methodology for Design Under Uncertainties Based on DACE Response Surface and Game Theory," *ERCOFTAC Bulletin*, Vol. 66, 2005, pp. 29–36.

[13] Garzon, V. E., and Darmofal, D. L., "Impact of Geometric Variability on Compressor Aerodynamic Performance," *Journal of Turbomachinery*, Vol. 125, No. 4, 2003, pp. 692–703.
doi:10.1115/1.1622715

[14] Lian, Y. S., and Kim, N. H., "Reliability-based Design Optimization of a Transonic Compressor," *AIAA Journal*, Vol. 44, No. 2, 2006, pp. 368–375.
doi:10.2514/1.16262

[15] Kumar, A., Keane, A. J., Nair, P. B., and Shahpar, S., "Robust Design of Compressor Fan Blades Against Erosion," *Journal of Mechanical Design*, Vol. 128, No. 4, 2006, pp. 864–873.
doi:10.1115/1.2202886

[16] Hicks, R. M., and Henne, P. A., "Wing Design by Numerical Optimization," *Journal of Aircraft*, Vol. 15, No. 7, 1978, pp. 407–412.
doi:10.2514/3.58379

[17] Sobol, I. M., "On the Systematic Search in a Hypercube," *SIAM Journal on Numerical Analysis*, Vol. 16, No. 5, 1979, pp. 790–793.
doi:10.1137/0716058

[18] Keane, A. J., "Comparison of Several Optimization Strategies for Robust Turbine Blade Design," *Journal of Propulsion and Power*, Vol. 25, No. 5, 2009, pp. 1092–1099.
doi:10.2514/1.38673

[19] Wiener, N., "The Homogeneous Chaos," *American Journal of Mathematics*, Vol. 60, No. 4, 1938, pp. 897–936.
doi:10.2307/2371268

[20] Cameron, R. H., and Martin, W. T., "The Orthogonal Development of Nonlinear Functionals in Series of Fourier-Hermite Polynomials," *Annals of Mathematics*, Vol. 48, No. 2, 1947, pp. 385–392.
doi:10.2307/1969178

[21] Ghanem, R., and Spanos, P., *Stochastic Finite Elements: A Spectral Approach*, Springer–Verlag, New York, 1991.

[22] Xiu, D., and Karniadakis, G. E., "The Wiener–Askey Polynomial Chaos for Stochastic Differential Equations," *SIAM Journal on Scientific Computing*, Vol. 24, No. 2, 2002, pp. 619–644.
doi:10.1137/S1064827501387826

[23] Le Maître, O. P., Reagan, M. P., Najm, H. N., Ghanem, R. G., and Knio, O. M., "A Stochastic Projection Method for Fluid Flow: Part I, Basic Formulation," *Journal of Computational Physics*, Vol. 173, No. 2, 2001, pp. 481–511.
doi:10.1006/jcph.2001.6889

[24] Choi, S. K., Grandhi, R. V., and Canfield, R. A., "Optimization of Stochastic Mechanical Systems Using Polynomial Chaos Expansion," *10th AIAA/ISSMO Multidisciplinary Analysis and Optimization Conference*, New York, 2004.

[25] Molina-Cristobal, A., Parks, G. T., and Clarkson, P. J., "Finding Robust Solutions to Multi-Objective Optimisation Problems Using Polynomial Chaos," *6th ASMO UK/ISSMO Conference on Engineering Design Optimization*, Oxford, 2006.

[26] Dodson, M., and Parks, G. T., "Robust Aerodynamic Design Optimization Using Polynomial Chaos," *Journal of Aircraft*, Vol. 46, No. 2, 2009, pp. 635–646.
doi:10.2514/1.39419

[27] Zhao, L., Dawes, W. N., Parks, G. T., Jarrett, J. P., and Yang, S., "Robust Airfoil Design with Respect to Boundary Layer Transition," 11th AIAA Non-Deterministic Approaches Conference, AIAA Paper 2009-2273, Palm Springs, CA, May 2009.

[28] Ghisu, T., Jarrett, J. P., and Parks, G. T., "Robust Design Optimization of Airfoils with Respect to Ice Accretion," *Journal of Aircraft*, Vol. 48, No. 1, 2011, pp. 287–304.
doi:10.2514/1.C031100

[29] Jakipse, D., and Platt, M. J., "Optimization in Component Design and Redesign," *10th International Symposium on Transport Phenomena and Dynamics of Rotating Machinery*, 2004.

[30] Ortiz-Dueñas, C., Miller, R. J., Hodson, H. P., and Longley, J. P., "Effect of Length on Compressor Inter-Stage Duct Performance," American Society of Mechanical Engineers, Paper GT 2007-27752, 2007.

[31] Jarrett, J. P., Dawes, W. N., and Clarkson, P. J., "An Approach to Integrated Multi-Disciplinary Turbomachinery Design," *Journal of Turbomachinery*, Vol. 129, No. 3, 2007, pp. 488–494.
doi:10.1115/1.2472416

[32] Ghisu, T., *Robust Aerodynamic Design of Compression Systems*, Ph.D. Thesis, Univ. of Cambridge, Cambridge, England, U.K., 2009.

[33] Molinari, M., *Reduced Order Modelling for Turbomachinery*, Ph.D. Thesis, Univ. of Cambridge, Cambridge, England, U.K., 2008.

[34] Jaeggi, D. M., Parks, G. T., Kipouros, T., and Clarkson, P. J., "The Development of a Multi-Objective Tabu Search Algorithm for Continuous Optimisation Problems," *European Journal of Operational Research*, Vol. 185, No. 3, 2008, pp. 1192–1212.
doi:10.1016/j.ejor.2006.06.048

[35] Glover, F., and Laguna, M., *Tabu Search*, Kluwer Academic, Norwell, MA, 1997.

[36] Hooke, R., and Jeeves, T. A., "'Direct Search' Solution of Numerical and Statistical Problems," *Journal of the Association for Computing Machinery*, Vol. 8, No. 2, 1961, pp. 212–229.
doi:10.1145/321062.321069

[37] Kroo, I., "Aeronautical Applications of Evolutionary Design," *Optimization Methods & Tools for Multicriteria/Multidisciplinary Design*, VKI Lecture Series, von Karman Inst. for Fluid Dynamics, Rhode-St-Genèse, Belgium, Nov. 2004.

[38] Kipouros, T., Jaeggi, D. M., Dawes, W. N., Parks, G. T., Savill, A. M., and Clarkson, P. J., "Biobjective Design Optimization for Axial Compressors Using Tabu Search," *AIAA Journal*, Vol. 46, No. 3, 2008, pp. 701–711.
doi:10.2514/1.32794

[39] Ghisu, T., Parks, G. T., Jarrett, J. P., and Clarkson, P. J., "The Benefits of Adaptive Parameterization in Multi-Objective Tabu Search Optimization," *Engineering Optimization*, Vol. 42, No. 10, Oct. 2010, pp. 959–981.
doi:10.1080/03052150903564882

[40] Nobile, F., Tempone, R., and Webster, C. G., "A Sparse Grid Stochastic Collocation Method for Partial Differential Equations with Random Input Data," *SIAM Journal on Numerical Analysis*, Vol. 46, No. 5, 2008, pp. 2309–2345.
doi:10.1137/060663660

[41] Smolyak, S. A., "Quadrature and Interpolation Formulas for Tensor Products of Certain Classes of Functions," *Doklady Akademii Nauk SSSR*, Vol. 148,1963, pp. 1042–1045.

[42] Hosder, S., Walters, R. W., and Balch, M., "Efficient Sampling for Non-Intrusive Polynomial Chaos Applications with Multiple Uncertain Input Variables," 48th AIAA/SME/ASCE/AHS/ASC Structures, Structural Dynamics and Materials Conference, Honolulu, AIAA Paper 2007-1939, 2007.

[43] Bell, T. A., Jarrett, J. P., and Clarkson, P. J., "Exploring the Effects of Removing Process-Intrinsic Constraints on Gas Turbine Design," *Journal of Propulsion and Power*, Vol. 24, No. 4, 2008, pp. 751–762.
doi:10.2514/1.34092

[44] Castillo, L., Wang, X., and George, W. K., "Separation Criterion for Turbulent Boundary Layers via Similarity Analysis," *Journal of Fluids Engineering*, Vol. 126, 2004, pp. 297–304.
doi:10.1115/1.1758262

[45] Jarrett, J. P., Ghisu, T., and Parks, G. T., "On the Coupling of Designer Experience and Modularity in the Aerothermal Design of Turbomachinery," *Journal of Turbomachinery*, Vol. 131, No. 3, 2009, Paper 031018.
doi:10.1115/1.2992513

[46] Huyse, L., and Lewis, R. M., "Aerodynamic Shape Optimization of Two Dimensional Airfoil Under Uncertain Conditions," NASA CR 210648, 2001.

F. Liu
Associate Editor